Spectroscopy and structural properties of amorphous and nanocrystalline silicon carbide thin films

Halindintwali, Sylvain; Knoesen, D.; Julies, B.A.; Arendse, C.J.; Muller, T.; Gengler, Régis Y.N.; Rudolf, P.; Loosdrecht, P.H.M. van

Published in:
Physica Status Solidi (C)

DOI:
10.1002/pssc.201084124

Publication date:
2011

Phys. Status Solidi C **8**, No. 9, 2661–2664 (2011) / **DOI** 10.1002/pssc.201084124

physica status solidi c
www.pss-c.com
current topics in solid state physics

Spectroscopy and structural properties of amorphous and nanocrystalline silicon carbide thin films

Sylvain Halindintwali[*, 1], D. Knoesen[1], B. A. Julies[1], C. J. Arendse[1], T. Muller[1], Régis Y. N. Gengler[2], P. Rudolf[2], and P. H. M. van Loosdrecht[2]

[1] University of the Western Cape, Private Bag X17, Bellville 7535, South Africa
[2] Zernike Institute for Advanced Materials, University of Groningen, 9747 AG Groningen, Netherlands

Received 3 October 2010, accepted 4 February 2011
Published online 1 June 2011

Keywords oscillator strength, excitonic transition, surface states, Γ-point

* Corresponding author: e-mail shalindintwali@uwc.ac.za, Phone: +27 21 959 3460, Fax: +27 21 959 3474

Amorphous SiC:H thin films were grown by hot wire chemical vapour deposition from a $SiH_4/CH_4/H_2$ mixture at a substrate temperature below 400 °C. Thermal annealing in an argon environment up to 900 °C shows that the films crystallize as μc-Si:H and SiC with a porous microstructure that favours an oxidation process. By a combination of spectroscopic tools comprising Fourier transform infrared, Raman scattering and X-rays photoelectron spectroscopy we show that the films evolve from the amorphous $SiH_x/SiCH_2$ structure to nanocrystalline Si and SiC upon annealing at a temperature of 900 °C. A strong RT photoluminescence peak of similar shape has been observed at around 420 nm in both as-deposited and annealed samples. Time-resolved luminescence measurements reveal that this peak is fast decaying with lifetimes ranging from 0.5 to ~1.1 ns.

1 Introduction Nanocrystalline silicon carbide material has attracted much attention due to its wide band gap, excellent thermal properties and large bonding energy rendering it ideal for optoelectronic applications in devices operating at high power levels and high temperatures [1-4]. Because of the aptitude of the hot wire chemical vapour deposition (HWCVD) to avail a high density of H radicals, crucial for nanocrystalline growth, this deposition has been used by many groups to produce nanocrystalline SiC at temperatures below 400 °C using monomethyl-silane (MMS) [3-6]. In this study we employed a $SiH_4/CH_4/H_2$ mixture to deposit amorphous silicon carbide (a-SiC:H) by HWCVD at a substrate temperature of 380 °C. Thermal annealing of the films in an Ar environment at 900 °C shows a phase change transition into nc-3C-SiC. Here, we focus on the optical and structural properties of these thin films, as revealed by a variety of spectroscopic tools, including Fourier transform infrared (FTIR), Raman, X-ray photoelectron (XPS) and photoluminescence (PL).

2 Experimental details

The samples used in this study were deposited onto Corning glass and c-Si (100) substrates kept at 380 °C; a Ta filament temperature of 1600 °C, and a process pressure of 100 Pa were used in a commercial HWCVD system described elsewhere [7]. The ratio between the CH_4 and SiH_4 flow rates (F) was fixed at 1.5, while the hydrogen dilution ratio in the SiH_4:CH_4 mixture was varied between 30 % and 80 %.

Table 1 Deposition conditions and some properties of the samples used in this study.

Sample	$F(SH_4)$ (sccm)	$F(CH_4)$ (sccm)	$F(H_2)$ (sccm)	Thickness (nm)	E_g (eV)	C_{Si-C} (at.%)
S_1	5.6	8.4	6	460	2.15	1.6
S_2	4	6	10	580	2.11	1.4
S_3	2.4	3.6	14	280	2.05	1.06
S_4	1.6	2.4	16	160	2.02	1.06

The thickness of the deposited layers was measured by a Veeco Dektak 6M profiler using the procedure described in [8]. Table 1 summarizes the deposition conditions.

FTIR absorption measurements were performed using a PerkinElmer Spectrum 100 spectrometer in the range from 400 to 4000 cm^{-1}. UV-VIS transmission spectra were recorded by a CARY 1E UV-visible spectrophotometer in the range between 400–900 nm. The PL experiments were performed at room temperature (RT) with a JOBIN YVON HORIBA double grating fluorologue FL3-22. For these experiments the samples were excited by a 430 W Xenon lamp at a wavelength of 320 nm. The spectra were collected by a cooled photomultiplier detector. Time resolved PL measurements were performed using a Hamamatsu C5680 series streak camera. In this case the excitation wavelength was 370 nm (the 2nd harmonic of a 100 fs Ti:Sapphire laser) with a power of 40 μW. The repetition rate was 1.9 MHz. The Raman measurements were taken using a 532.06 nm green laser line with an excitation power of 1.2 mW. The signal was recorded by a CCD-detector cooled at -135 °C. X-ray photoelectron spectroscopy (XPS) data were collected using a Surface Science SSX-100 ESCA instrument equipped with a monochromatic Al K_α X-ray source ($h\nu$ = 1486.6 eV). The takeoff angle between the spectrometer detector and the normal to the surface was 37°. Binding energies (± 0.1 eV) were referenced to the silicon 2p photoemission line at a binding energy of 99.3 eV [9].

3 Results and discussion

3.1 Optical properties Figure 1 shows the optical absorption spectra of the as-deposited samples, demonstrating a clear increase of the absorption band edge upon increasing CH_4 flow rate. This is also demonstrated by the optical band gap (E_g) values calculated by the Tauc model from the absorption data (see Tab. 1) using the procedure discussed in [10]. The obtained values range between 2.02 eV for the lowest flow to 2.15 eV for the highest. The origin of this widening of the band gap is assigned to the incorporation of carbon into the films. The values obtained are close to the room temperature (RT) band gap of 3C-SiC (2.2 eV). In addition, we found that the refractive indices derived using the Tauc model (n = 2.52 – 2.54) are also characteristic of SiC related material.

3.2 Structural properties The structural properties have been studied by XPS, FTIR and Raman scattering spectroscopy. Figure 2 shows typical XPS spectra of the films under study. While the main spectrum in Fig. 2 confirms that the film is composed of Si, C and O, the insert shows that the Si 2p peak (spin-orbit doublet not resolved) can be separated into two components at ~100 eV and 103 eV binding energy associated with Si bound into SiC and Si bound into silanes and/or SiO_x, respectively [9]. The O 1s core level line is observed at a binding energy typical of a Si-O-Si bond [11], namely at around 533 eV for the as-deposited films; it shifts to around 534 eV in the spectra of the annealed films. This shift to higher binding energy is attributed to local structural readjustements of Si oxide resulting from the complete effusion of hydrogen relieving the films from strained bonds formed during crystallization. This blue shift has been previously reported in nanoporous Si oxide [11].

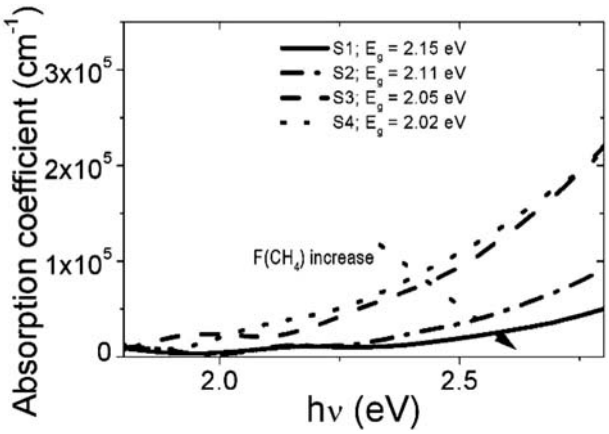

Figure 1 Absorption spectra of the as-deposited samples. The absorption edge blue shifts with the increase of the methane flow as shown by the dotted arrow on the figure.

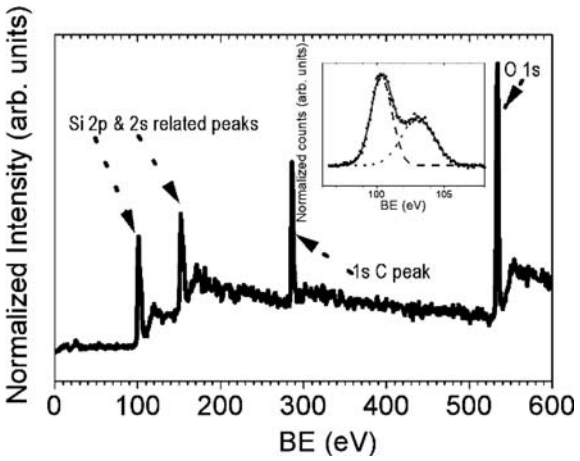

Figure 2 X-ray photoelectron spectrum of an as-deposited sample showing the signature of Si, C and O in the films. The insert shows a splitting of the silicon 2p core level peak implying different bonding configuration.

Figure 3 shows the IR spectra of an as-deposited (lower curve) and annealed (upper curve) sample. The spectrum of the as-deposited sample shows the characteristic features corresponding to $(SiH_2)_n$ rocking/wagging and SiH_2 bending modes at 630 cm^{-1} and 872 cm^{-1} respectively [12]. The peaks at 790 cm^{-1} and around 1000 cm^{-1} correspond to Si-C stretching and C-H_2 (within $SiCH_2$) wagging vibrations, respectively [13]. In addition to this, the 1000 cm^{-1} peak shows a clear broadening towards higher energy which is a typical signature of oxidation, consistent with the XPS results. The spectrum of the annealed sample (900

°C for 30 minutes) shows a complete disappearance of the SiH_n vibration bonds at 630 $cm^{-1}$and 872 cm^{-1}. This may be explained by the effusion of hydrogen from a-Si:H matrix; one expects complete H_2 effusion from bulk a-Si:H film already for annealing temperatures below 600 °C [14]. Moreover the Si-C stretching vibration modes at 790 cm^{-1} broadens and includes a component at around 800 cm^{-1} while the 1000 cm^{-1} peak is seen to shift to higher energy.

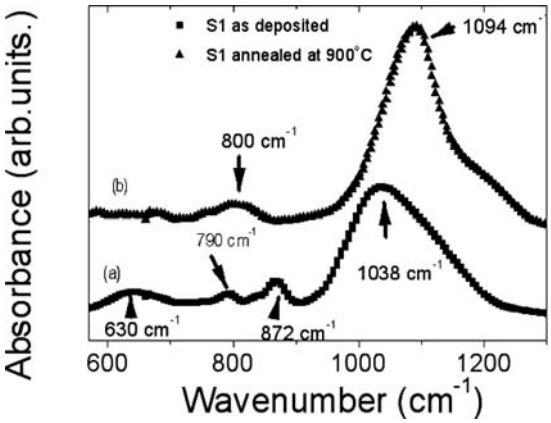

Figure 3 Typical FTIR spectra of the films in as-deposited (a) and annealed films (b).

The component at around 800 cm^{-1} can be attributed to the formation of SiC nanocrystals in the films on annealing while the shift of the 1000 cm^{-1} peak to higher energy indicates that the hydrogen atoms that were bonded as $C-H_2$ within $SiCH_2$ have effused from the material; the microstructure becomes porous. While the carbon atoms that were bonded in $SiCH_n$ evolve on annealing into SiC stretching bonds as detected at 800 cm^{-1} by FTIR, the low intensity of this peak suggests however that most of the Si atoms that were part of these bonds as well as those that were bonded as SiH_n at 630 cm^{-1} in the as-deposited films crystallize into Si-Si on annealing. Using the oscillator strength $A_{Si-C} = 2.13 \times 10^{19}$ cm^{-2} [13] and assuming that the network is mainly composed of Si atoms we have quantified the content of Si-C, C_{Si-C} between 1 and 1.6 at. % (Tab. 1, 7th column). This is supported by the Raman scattering spectra. While the as-deposited films showed spectra typical for amorphous films by the presence of a broad band between 400 and 500 cm^{-1} (the data are not shown here), the spectra of the annealed films showed a fairly flat spectrum in this region and only the presence of the sharp 520 cm^{-1} peak typical for Si-Si vibrations (Fig. 4). This change in spectra was only observed for annealing temperatures above 800 °C. An emergence of a microcrystalline silicon structure in the films grown at high hydrogen dilution ratio is seen in the two bottom spectra. It is apparent that the growth of μc-Si at this stage is suppressed in the films deposited with a high flow of methane in the two top spectra; this is explained by the fact that the C-H bonds have higher bond energy than their Si-H counterparts, which promotes a better thermal stability of the films with respect to hydrogen effusion.. The spectra of the films annealed at 900 °C are characterized by a sharp prominent peak at 520 cm^{-1} due to crystalline Si and a small broad peak centred around 960 cm^{-1} attributed to 3C-SiC LO phonons [15, 16].

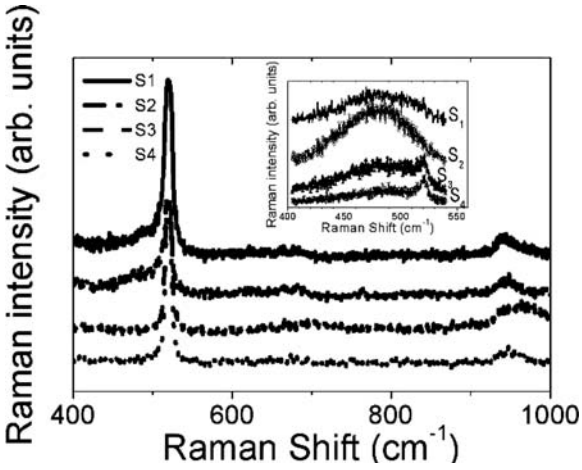

Figure 4 Raman spectra of the films annealed at 900 °C; the insert displays the spectra of the films annealed at 800 °C.

3.3 Luminescence properties Figure 5 shows the major peak observed in the RT PL spectra of the as-deposited films. The insert displays the spectra of the same films when annealed at 800 °C. The shape and position of the peaks, centred around 2.95 eV are similar in both series. The energy of this emission is higher than the bandgap of the material (see Table 1) on one hand but lower than the 3.2 eV direct transition at the Γ-point in bulk Si on the other hand. We therefore assign this to a transition arising from the Si network in the films.

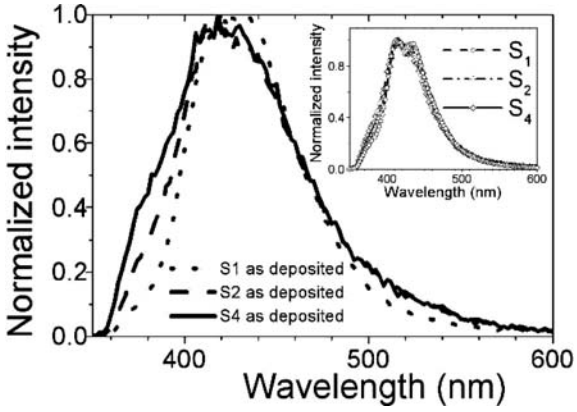

Figure 5 Typical room temperature PL spectra observed in the films as deposited; the insert displays the spectra of the annealed films at 800 °C.

The dynamics of this peak have been examined by time resolved PL. Figure 6 displays a typical time-resolved PL spectrum of sample S_2 annealed at 800 °C. Since the luminescence intensity is proportional to the time-derivative of the e-h (electron-hole) pair density whose decay follows

the streched exponential function, we fit the experimental data using an equation of the the form [17]

$$I(t) = A \times t^{\alpha-1} \times \exp[-(\frac{t}{\tau})^{\alpha}] \qquad (1)$$

where I(t) and A are the PL intensity during the decay and a pre-factor, respectively. α and τ are characteristic constants of the decay, α being related to the amount of „stretching" during the decay [18]. A small value of α indicates a rapid decay in the early time [19] and was ≅ 0.9 in our fitting procedure.

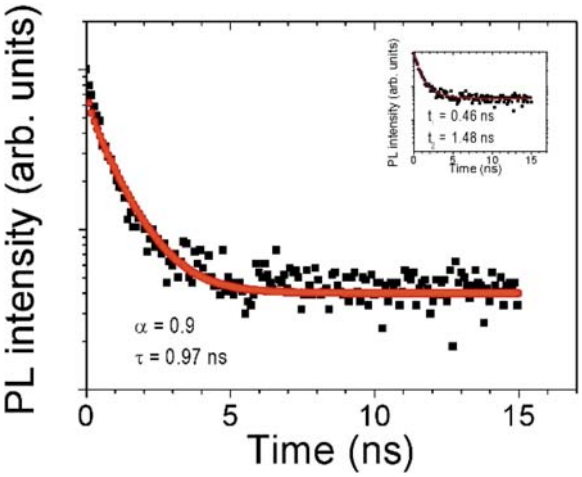

Figure 6 Time-resolved decay spectrum of sample S_2 annealed at 800 °C (semi-logarithmic scale) fitted by a stretched exponential (main graph); the fit in the insert follows a two exponential decay.

The time characteristic τ in the samples was found in the range between 0.5 – 1.1 ns. This direct transition is faster than the bound excitonic transition in bulk 3C-SiC [20] and the often reported radiative recombination of electrons localized at oxygen-related states at Si/SiO_2 interface [21]. It is difficult to discriminate between this stretched fit and a two exponential decay (in the insert) where the two exponential decay times could come from bulk vs surface, or from different types of surface states.

4 Conclusion a-SiC:H films have been deposited by the HWCVD at a temperature of the substrate below 400 °C. Using a variety of spectroscopy techniques, it is shown that a thermal annealing up to 900 °C induces a nanoporous Si/SiC structure prone to oxidation. Such microstructure is responsible of a strong RT luminescence emission that decays fast in time. The fitting of the data with a stretched exponential function yields lifetime values generally lower than 1 ns. In-depth studies are underway for a proper assignment of this fast band transition.

Acknowledgements Sylvain Halindintwali acknowledges the COIMBRA scholarship for young Africans scientists that funded a research visit to the University of Groningen. The following people are acknowledged for their technical support in their respective capacities: Ben Hesp, Foppe de Haan, Arjen Kamp, Jakob Baas of the University of Groningen and Timothy Lesch of the University of Western Cape.

References

[1] V. M. Ng, M. Xu, S. Y. Huang, J. D. Long, and S. Xu, Thin Solid Films **506/507**, 283-287 (2006).
[2] A. Tabata, Y. Komura, T. Narita, and A. Kondo, Thin Solid Films **517**, 3516-3519 (2009).
[3] S. Klein, R. Carius, F. Finger, and L. Houben, Thin Solid Films **501**, 169-172 (2006).
[4] S. Miyajima, K. Haga, A. Yamada, and M. Konagai, Jpn. J. Appl. Phys. **45**, 432 (2006).
[5] T. Kaneko, Y. Hosokawa, T. Suga, and N. Miyakawa, Microelectron. Eng. **83**, 41 (2006).
[6] T. Kunii, T. Honda, N. Yoshida, and S. Nonomura, J. Non-Cryst. Solids **352**, 1196 (2006).
[7] S. Halindintwali, D. Knoesen, R. Swanepoel, B. A. Julies, C. Arendse, T. Muller, C. C. Theron, A. Gordijn, P. C. P. Bronsveld, J. K. Rath, and R. E. I. Schropp, Thin Solid Films **515**, 8040-8044 (2007).
[8] S. Halindintwali, D. Knoesen, R. Swanepoel, B. A. Julies, C. Arendse, T. Muller, C. C. Theron, A. Gordjin, P. C. P. Bronsveld, J. K. Rath, and R. E. I. Schropp, South Afr. J. Sci. **105**, 290-293 (2009).
[9] J. F. Moulder, W. F. Stickle, P. E. Sobol, K. D. Bomben, Handbook of X-ray Photoelectron Spectroscopy, edited by Jill Chastain and Roger C. King, Jr. (Physical Electronics, Inc., 6509 Flying Cloud Drive, Eden Prairie, Minnesota 55344, USA).
[10] S. Halindintwali, D. Knoesen, T. F. G. Muller, D. Adams, N. Tile, C. C. Theron, and R. E. I. Schropp, J. Mater. Sci. Mater. Electron. **18**, S225-S229 (2007).
[11] M. T. K. Soh, J. H. Thomas, and J. J. Talghader, J. Vac. Sci. Technol. A **24**, 2147-50 (2006).
[12] W. S. Lau, Infrared Characterization of Microelectronics (World Scientific, Singapore, 1999).
[13] T. Kaneko, D. Nemoto, A. Horiguchi, and N. Miyakawa, J. Cryst. Growth **275**, e1097-e1101 (2005).
[14] H. Ohmi and K. Yasutake, Appl. Phys. Lett. **91**, 241901 (2007).
[15] S. Klein, L. Houben, R. Carius, F. Finger, and W. Fischer, J. Non-Cryst. Solids **352**, 1376-1379 (2006).
[16] R. Dutta, P. K. Banerjee, and S. S. Mitra, Phys. Rev. B **27**, 5032 (1983).
[17] T. Aoki, K. Ikeda, S. Kobayashi, and K. Shimakawa, Philos. Mag. Lett. **86**, 137 (2006).
[18] J. Linnros, A. Galeckas, N. Lalic, and V. Grivickas, Thin Solid Films **297**, 167-170 (1997).
[19] K. Morigaki, Phys. Status Solidi A **206**(5), 868-873 (2009); DOI 10.1002/pssa.200881324.
[20] M. B. Yu. Rusli, S. F. Yoon, S. J. Xu, K. Chew, J. Cui, J. Ahn, and Q. Zhang, Thin Solid Films **377/378**, 177-181 (2000).
[21] A. A. Prokofiev, A. S. Moskalenko, I. N. Yassievich, W. D. A. M. de Boer, D. Timmerman, H. Zhang, W. J. Buma, and T. Gregorkiewicz, Pis′ma v ZhETF **90**(12), 856-860 (2009).

